Biophysical Journal Volume 104 February 2013 835–840

Biophysical Model of Bacterial Cell Interactions with Nanopatterned Cicada Wing Surfaces

Sergey Pogodin,[†] Jafar Hasan,[‡] Vladimir A. Baulin,[†§*] Hayden K. Webb,[‡] Vi Khanh Truong,[‡] The Hong Phong Nguyen,[‡] Veselin Boshkovikj,[‡] Christopher J. Fluke,[¶] Gregory S. Watson,[‖] Jolanta A. Watson,[‖] Russell J. Crawford,[‡] and Elena P. Ivanova[‡*]

[†]Departament d'Enginyeria Quimica, Universitat Rovira i Virgili, Tarragona, Spain; [‡]Faculty of Life and Social Sciences and [¶]Centre for Astrophysics and Supercomputing, Swinburne University of Technology, Hawthorn, Victoria, Australia; [§]Institució Catalana de Recerca i Estudis Avançats, Barcelona, Spain; and [‖]Centre for Biodiscovery and Molecular Development of Therapeutics, School of Marine and Tropical Biology, James Cook University, Townsville, Queensland, Australia

ABSTRACT The nanopattern on the surface of Clanger cicada (*Psaltoda claripennis*) wings represents the first example of a new class of biomaterials that can kill bacteria on contact based solely on their physical surface structure. The wings provide a model for the development of novel functional surfaces that possess an increased resistance to bacterial contamination and infection. We propose a biophysical model of the interactions between bacterial cells and cicada wing surface structures, and show that mechanical properties, in particular cell rigidity, are key factors in determining bacterial resistance/sensitivity to the bactericidal nature of the wing surface. We confirmed this experimentally by decreasing the rigidity of surface-resistant strains through microwave irradiation of the cells, which renders them susceptible to the wing effects. Our findings demonstrate the potential benefits of incorporating cicada wing nanopatterns into the design of antibacterial nanomaterials.

INTRODUCTION

Several surfaces exist in nature that are capable of maintaining a contaminant-free status despite the innate abundance of potential contaminants in their surrounding environments (1–5). The vast majority of these surfaces owe their self-cleaning qualities to their superhydrophobic properties, which in turn are largely due to their physical surface structure. Many animals (e.g., sharks (6,7), cicadae (8), butterflies (9), termites (10), mosquitos (11), and geckos (12)) and plants (e.g., lotus (*Nelumbo nucifera*) (13,14) and cabbage (*Brassica oleracea*) (15)) possess hierarchical surface features that significantly increase their hydrophobicity, often to the point of becoming superhydrophobic (10,16).

A number of research groups have attempted to establish a direct link between the self-cleaning and antibiofouling properties of surfaces, i.e., the ability to prevent attachment and accumulation of biological material (17–20). More recently, we demonstrated that superhydrophobic/self-cleaning surfaces are not necessarily inherently antibiofouling in nature (8). *Pseudomonas aeruginosa* cells were found to be capable of adhering relatively effectively onto the surface of the wings of the Clanger cicada (*Psaltoda claripennis*); however, those cells that were able to attach to the surface were killed with extreme efficiency by the wing surface (8). We further demonstrated that cicada wings were efficient at killing other Gram-negative bacteria (i.e., *Branhamella catarrhalis*, *Escherichia coli*, and *Pseudomonas fluorescens*), whereas Gram-positive bacteria (*Bacillus subtilis*, *Pseudococcus maritimus*, and *Staphylococcus aureus*) remained resistant (21). This result suggests that a common mechanism underlies the observed phenomenon. Even more significantly, we also demonstrated that the bactericidal properties of the wings took the form of a mechanical rupture of the bacteria arising from physical interactions between the cells and the nanoscale wing surface structure. To our knowledge, these cicada wings were the first described example of a surface that possesses biocidal activity based solely on its physical surface structure (8).

The antibacterial properties of cicada wings have only very recently been discovered, and hence there is still much to be learned about the specific mechanisms that lead to the observed bactericidal behavior (8,21). It is critical to obtain a greater fundamental understanding of these mechanisms before any attempt can be made to apply these structures in medical contexts. We developed a biophysical model to provide insight into the interactions that take place between the bacterial cells and the cicada wing surface structures. Adsorption of the bacterial cell membrane on the pattern of the cicada wing surface may lead to a drastic increase of the total area, accompanied by stretching of the membrane, which may in turn lead to irreversible membrane rupture and death of bacteria. Previously, gold coating of cicada wings was shown to significantly alter the surface properties while preserving both the topographical structure and subsequently the bactericidal effect (8). This observation led to two research hypotheses that are the focus of this work: 1), the mechanism is biophysical and no specific biological interactions play a role; and 2), less rigid bacterial membranes will be more affected by the bactericidal mechanism of the wings.

Submitted August 10, 2012, and accepted for publication December 31, 2012.

*Correspondence: vladimir.baulin@urv.cat or eivanova@swin.edu.au

Editor: Simon Scheuring.

0006-3495/13/02/0835/6 $2.00

http://dx.doi.org/10.1016/j.bpj.2012.12.046

MATERIALS AND METHODS

Sample preparation

Cicada (*P. claripennis*) specimens were collected from the greater Brisbane parkland areas. It is known that the cell regions of the dorsal and ventral sides of the wings possess a homogeneous nanopattern on their surface (22). For consistency, all experiments were performed on the same cell regions on the dorsal side of the forewing. Portions of the wings (~0.5 cm × 0.5 cm) were excised by a scalpel or scissors and attached onto circular coverslips with adhesive tape. The wing samples were then briefly rinsed with MilliQ H_2O (resistivity of 18.2 MΩ cm^{-1}; Millipore, Billerica, MA) and finally blow-dried with nitrogen gas (99.99% purity) (23).

Scanning electron microscopy

High-resolution scanning electron microscopy (SEM) images of cicada wings with adhering bacteria were taken with the use of a field-emission scanning electron microscope (Supra 40 VP; Zeiss, Oberkochen, Germany) at 3 kV under 35,000× and 42,000× magnification. Samples were coated with thin gold films using a Dynavac CS300 before they were viewed with the microscope.

Atomic force microscopy

Atomic force microscopy (AFM) scans were performed with an Innova microscope (Veeco/Bruker, Santa Barbara, CA) as described elsewhere (8). Briefly, scans were conducted using phosphorus-doped silicon probes (MPP-31120-10; Veeco/Bruker) with a spring constant of 0.9 N/m, tips with radius of curvature of 8 nm, and a resonance frequency of ~20 kHz for surface imaging. Scanning was carried out in tapping mode perpendicular to the axis of the cantilever at 1 Hz.

Bacterial strains, growth, and sample preparation

Bacillus subtilis NCIMB 3610T, *Planococcus maritimus* KMM 3738, and *Staphylococcus aureus* CIP 65.8T were used in this study. Bacterial strains were obtained from the National Collection of Industrial, Food and Marine Bacteria (NCIMB, Aberdeen, UK), the Collection of Marine Bacteria (KMM, Russian Federation), and the Culture Collection of the Institute Pasteur (CIP, France). Before each experiment, bacterial cultures were refreshed from stocks on nutrient agar (Oxoid, UK) or marine agar (BD). For cell attachment experiments, fresh bacterial suspensions were prepared for each strain grown overnight at 37°C in 5 mL of nutrient broth (Oxoid) or at 25°C in 5 mL of marine broth (Difco) with shaking (120 rpm). Bacterial cells were collected at the logarithmic stage of growth and the suspensions were adjusted to $OD_{600} = 0.3$ as described elsewhere (8). The mounted insect wings were immersed in 5 mL of the bacterial suspension and incubated for 18 h.

Confocal laser scanning microscopy

Live and dead bacterial cells were visualized and differentiated using a FluoView FV10i inverted confocal laser scanning microscopy (CLSM) system (Olympus, Tokyo, Japan). Cells were stained using the LIVE/DEAD *Bac*Light Bacterial Viability Kit, L7012, which contains a mixture of SYTO 9 and propidium iodide fluorescent dyes (Molecular Probes/Invitrogen, NY) according to the manufacturer's protocol. SYTO 9 permeates all cells, binding to DNA and causing a green fluorescence. Propidium iodide only enters cells that have significant membrane damage, which is an indication of nonviability, and binds to nucleic acids with higher affinity than SYTO 9.

Microwave experiments

Bacterial samples for microwave (MW) treatment were comprised of 2 mL of cell suspensions ($OD_{600} = 0.1$) that were transferred into a micro Petri dish (35 mm i.d.; Greiner Bio-One, Frickenhausen, Germany). The MW apparatus was a Lambda Technologies Vari-Wave model LT 1500 with the frequency fixed at 18 GHz and other settings as described elsewhere (24). The bulk temperature of the bacterial suspension during exposure was controlled to remain below 40°C at all times. Each sample was exposed to MW radiation for three consecutive exposures of 1 min each, and the sample was allowed to cool back down to 20°C between exposures. After treatment, the cell suspensions were incubated on insect wings mounted on circular coverslips in the same manner employed for the untreated cells.

RESULTS AND DISCUSSION

The surface structure of the wings of *P. claripennis* has been extensively characterized by AFM and SEM imaging techniques and described in earlier reports (8,21–23). We confirmed that the wing surfaces were covered by an array of nanopillar structures arranged approximately hexagonally, spaced 170 nm apart from center to center (Fig. 1). Each pillar was ~200 nm tall, with a conical shape and a spherical cap 60 nm in diameter.

Pseudomonas aeruginosa ATCC 9027 bacterial cells in contact with cicada wings are known to be deformed and

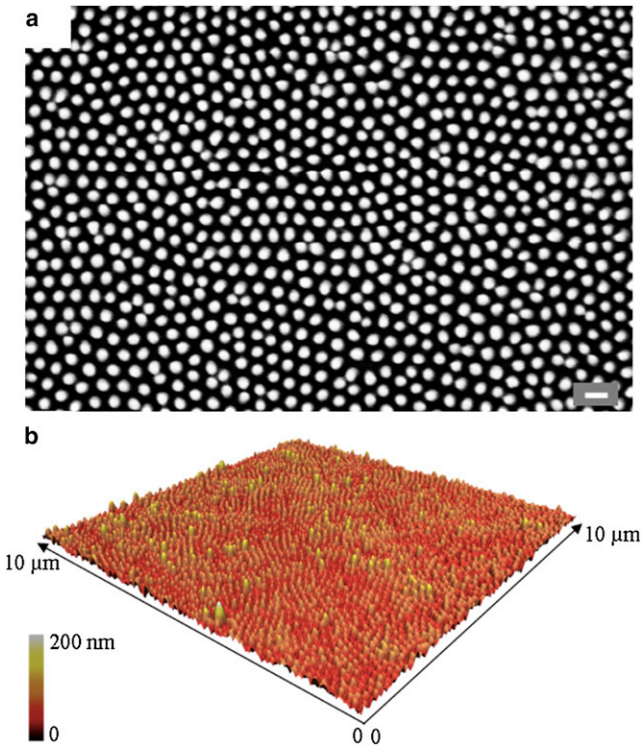

FIGURE 1 Cicada (*P. claripennis*) wing surface topography. (*a*) Scanning electron micrograph of the surface of a cicada wing as viewed from above (scale bar = 200 nm). (*b*) Three-dimensional representation of the surface architecture of a cicada wing, constructed from AFM scan data and colored according to height. A three-dimensional animation of the cicada wing surface is available at http://youtu.be/JDOEAUdqJGk.

mechanically ruptured by the nanopattern on the surface of the wing (8). Because the characteristic dimensions of the nanopillars on the surface of the cicada wings (~100 nm) are an order of magnitude larger than the thickness of the bacterial membrane (~10 nm) (25), we can model the membrane as a thin elastic layer and neglect the details of the structure and composition of the layer. Similarly, because the typical size of a bacterial cell (i.e., ~500–1000 nm) is at least several times larger than the spacing between the nanopillars, we can also ignore the curvature of the bacterial surface in the first approximation and limit our consideration to the adsorption of a planar piece of a membrane onto an array of nanopillars. In our model, the increase of the total area due to adsorption on the pillars leads to nonuniform stretching due to a specific surface pattern, which in turn leads to membrane rupture.

In such a macroscopic description, the bacterial outer layer is characterized by the stretching modulus (k), the surface density of the attraction sites on the relaxed layer (n_0), and the energy gain per adsorption site (ε). The microscopic nature of the attraction forces between the layer and the nanopillars is concealed into a single parameter ε, thus providing a certain degree of universality. The stretching of the layer due to the adsorption is described by the local relative stretching degree $\alpha(r)$ at point r. We assume that the unperturbed membrane is characterized by the total area S_i, the initial stretching α_i and initial uniform density n_0 of the adsorption sites. The stretching due to contact with pillars on the surface of the cicada wings leads to the redistribution of the adsorption sites from n_0 to the local density $n(r) = n_0/(1 + \alpha(r))$. Each site that is adsorbed on the nanopillar surface contributes the energy gain ε; therefore, the total free energy gain due to the adsorption is given by

$$F^{gain} = \int_A \varepsilon n(\mathbf{r}) d\boldsymbol{\sigma} = \int_A \frac{\varepsilon n_0 d\boldsymbol{\sigma}}{1 + \alpha(\mathbf{r})}, \quad (1)$$

where $d\sigma$ is an element of the layer surface area, and the integration is performed over the total contact area between the layer and the nanopillar surface (A).

The energy gain due to adsorption on the nanopillars is balanced by the free-energy loss associated with deformation of the membrane. The main contribution to the energy loss, F^{loss}, is due to local membrane stretching/compression, which is proportional to $(k/2)\alpha^2(r)$ for weak local deformations, $|\alpha(r)| \ll 1$. Thus, the integration over the total adsorbed area of the layer (A) plus the total area of the layer suspended between the nanopillars (B) gives

$$F^{loss} = \int_{A+B} \frac{k}{2}\alpha^2(\mathbf{r}) \frac{n(\mathbf{r})}{n_0} d\boldsymbol{\sigma} = \int_{A+B} \frac{k}{2}\alpha^2(\mathbf{r}) \frac{d\boldsymbol{\sigma}}{1 + \alpha(\mathbf{r})}. \quad (2)$$

The local stretching $\alpha(r)$ is not a completely independent variable. It relates the unperturbed area before adsorption and the area stretched due to adsorption through the following geometrical condition: the projection of unperturbed and stretched areas on the surface plane remains constant. This condition can be taken into account in the total free energy with the help of the Lagrange multiplier λ:

$$F = F^{gain} + F^{loss} + \lambda k \left(\int_{A+B} \frac{d\boldsymbol{\sigma}}{1 + \alpha(\mathbf{r})} - S_0 \right), \quad (3)$$

where S_0 is the initial area prior to contact with pillars. Minimization of this expression with respect to $\alpha(r)$ yields the local stretching of the layer in region A, where the membrane interacts with the nanopillars, and region B, where the membrane is suspended between pillars, leading to the following condition:

$$1 + \alpha(r) = \begin{cases} 1 + \alpha_A = \sqrt{1 + 2(\lambda - \zeta)}, & \text{region A} \\ 1 + \alpha_B = \sqrt{1 + 2\lambda}, & \text{region B} \end{cases} \quad (4)$$

where the dimensionless effective interaction parameter $\zeta \equiv -\varepsilon n_0/k$ is defined as the ratio between the attraction of the layer to the nanopillar surface and the layer elasticity. Equation 4 leads to an important general conclusion. In the case in which adsorption ε is negative and hence ζ is positive, the stretching of the suspended region of the layer, α_B, is higher than the stretching of the adsorbed region of the layer, α_A. This means that the rupture point of the layer will always be reached first in region B. In other words, the nanopillars do not pierce the membrane, but rather break the membrane between the nanopillars. One might imagine a scenario in which the nanopillars pierce the layer like an array of needles; however, this would only be the case if the diameter of the spherical caps were much smaller than is actually the case, e.g., ~1 nm as opposed to the measured 60 nm.

Because α_A and α_B are constant for all points inside regions A and B, respectively, we can simplify Eq. 3 by converting the integrals into areas S_A and S_B of the corresponding regions of the layer:

$$F = \frac{\varepsilon n_0 S_A}{1 + \alpha_A} + \frac{k}{2}\left(\frac{\alpha_A^2 S_A}{1 + \alpha_A} + \frac{\alpha_B^2 S_B}{1 + \alpha_B} \right) + \lambda k \left(\frac{S_A}{1 + \alpha_A} + \frac{S_B}{1 + \alpha_B} - \frac{S_i}{1 + \alpha_i} \right). \quad (5)$$

Here we consider that the unperturbed membrane is stretched up to the initial stretching degree, α_i, and the total initial area of unperturbed membrane is S_i.

The geometry of the nanopattern on the surface of cicada wings is described by four parameters (Fig. 2 *a*): the radius of the cap on top of the pillar ($R = 30$ nm), the pillar height ($h = 200$ nm), the pillar pitch ($\beta = 10^\circ$), and the average distance between the pillars ($d = 170$ nm). Assuming that

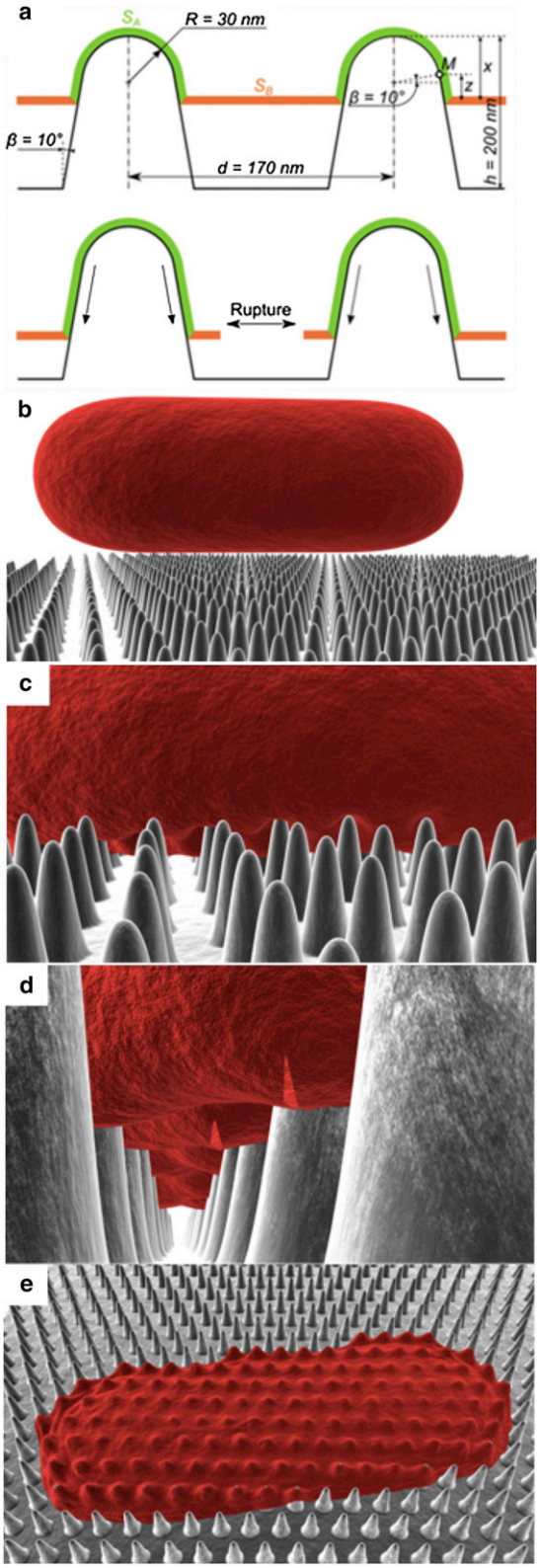

FIGURE 2 Biophysical model of the interactions between cicada (*P. claripennis*) wing nanopillars and bacterial cells. (*a*) Schematic of a bacterial outer layer adsorbing onto cicada wing nanopillars. The adsorbed layer can be divided into two regions: region A (in contact with the pillars) and region B (suspended between the pillars). Because region A adsorbs and the surface area of the region (S_A) increases, region B is stretched and eventually ruptures. (*b–e*) Three-dimensional representation of the modeled interactions between a rod-shaped cell and the wing surface. As the cell comes into contact (*b*) and adsorbs onto the nanopillars (*c*), the outer layer begins to rupture in the regions between the pillars (*d*) and collapses onto the surface (*e*). Images *b–e* are screenshots from an animation of the mechanism available at http://youtu.be/KSdMYX4gqp8.

the membrane suspended between the pillars (region B) remains horizontal with respect to the plane of the wing, the membrane position can be characterized by a single parameter: the vertical distance x from region B to the tip of the nanopillars. It is also convenient to consider separately two cases, in which region B is above (case I) and below (case II) the junction point M between the spherical cap and conical column of the nanopillar (Fig. 2 *a*). In case I, it is more convenient to describe the position of the layer by the angle θ between the nanopillar vertical axis and the contact point between the nanopillar and region B of the layer. In case II, the most convenient parameter is the vertical distance z between region B and the junction point M. Assuming that the average initial area of the layer per nanopillar is $S_i = d^2$, the areas S_A and S_B are given by the following expressions:

$$\left.\begin{aligned} S_A &= 2\pi R^2(1-\cos\theta) \\ S_B &= d^2 - \pi R^2 \sin^2\theta \end{aligned}\right\} \quad \text{case I}$$

$$\left.\begin{aligned} S_A &= 2\pi R^2(1-\sin\beta) + \frac{2\pi z}{\cos\beta}\left(R\cos\beta + \frac{z}{2}\tan\beta\right) \\ S_B &= d^2 - \pi(R\cos\beta + z\tan\beta)^2 \end{aligned}\right\} \quad \text{case II} \tag{6}$$

These expressions allow for numerical minimization of the free energy, which gives the equilibrium position and the equilibrium stretching of the membrane. Fig. 3 *a* shows the calculated dependencies of the membrane stretchings, α_A (region A) and α_B (region B), on the effective interaction parameter, ζ, for different values of the initial degree of stretching, α_i. It was found that α_B increases continuously as ζ increases. This suggests that there is a critical value, $\zeta_{critical}$, of the layer parameter, ζ, at which α_B also reaches a critical value and the membrane is ruptured.

The model suggests that the bactericidal mechanism is biophysical and does not imply directly any specific biological interactions. This is consistent with a previous experiment in which cicada wing surfaces were coated with gold (8). This technique preserves the geometry of the wings but changes the surface properties. The result demonstrates that such a pattern is lethal for *P. aeruginosa* cells, despite the substantial difference in surface chemistry. To explore the predictions of the proposed model and check the universality of the mechanism, we investigated the attachment behavior of two species of Gram-positive cocci, *Planococcus maritimus* and *S. aureus*, and the Gram-positive, rod-shaped bacterium *Bacillus subtilis* on cicada wing

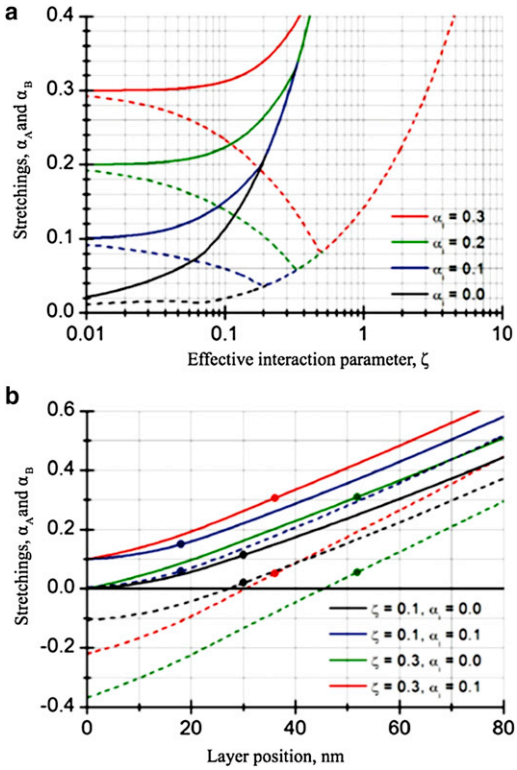

FIGURE 3 Modeled stretching dynamics of the outer layer of a bacterial cell in contact with a cicada wing surface. (*a*) Stretching in region A (α_A, *dashed lines*) and region B (α_B, *solid lines*) is plotted as a function of the layer parameter ζ for layers under different degrees of initial stretching (α_i), denoted by color. (*b*) Stretching in α_A and α_B is plotted as a function of the position of the layer relative to junction point *M* between the spherical cap and conical base of the nanopillars. Both α_A and α_B are plotted for different combinations of ζ and α_i. The equilibrium position of the layer in each case is marked with a dot.

surfaces (21). It is well documented that Gram-positive bacteria are generally more rigid than their rod-shaped counterparts, mostly due to the larger proportion of peptidoglycan present in the cell wall (25–27). Therefore, we performed comparative attachment experiments to determine whether Gram-positive cells respond in a similar manner to the Gram-negative *Pseudomonas aeruginosa*. The results of this experiment revealed that all three species were unaffected by the nanopillar structures on the wing surface. Scanning electron micrographs showed clearly that the cells retained their characteristic morphologies, and CLSM confirmed that the cells remained viable. According to the model, the effective interaction parameter ζ is proportional to the attraction between the bacterial layer and the wing surface, and is inversely proportional to the layer rigidity. Thus, more rigid cells require a stronger interaction with the surface to sufficiently stretch to the point of rupture. This offers a possible explanation for the resistance of *B. subtilis*, *Planococcus maritimus*, and *S. aureus* against the action of the cicada wings, in that they possess increased rigidity relative to *Pseudomonas aeruginosa* (25–27).

If the presented model stands, one would expect that if the cell rigidity is decreased and/or the initial stretching on the membrane is sufficiently decreased, the bacterial strains that were previously resistant to the bactericidal action of the wing surface could potentially become susceptible. MW exposures under specified conditions were previously shown to induce reversible poration in the membranes of bacteria (28,29), allowing the release of some of the cellular contents, decreasing internal turgor pressure, and releasing some of the tension on the membrane. However, this technique itself is not lethal to the cells, and the pores in the membranes self-seal after a few minutes. To test our theory, we exposed cells of *B. subtilis*, *Planococcus maritimus*, and *S. aureus* to MW radiation and then incubated them in the presence of cicada wings. The morphology of irradiated cells that came into contact with the wing surface was markedly different from that of the nonirradiated cells (Fig. 4, *left*). The MW-treated cells were considerably deformed by the nanopillars, in a manner similar to that observed for the untreated *Pseudomonas aeruginosa* (8), confirming that the decrease in turgor pressure induced by the MW treatment had rendered these cells susceptible to the

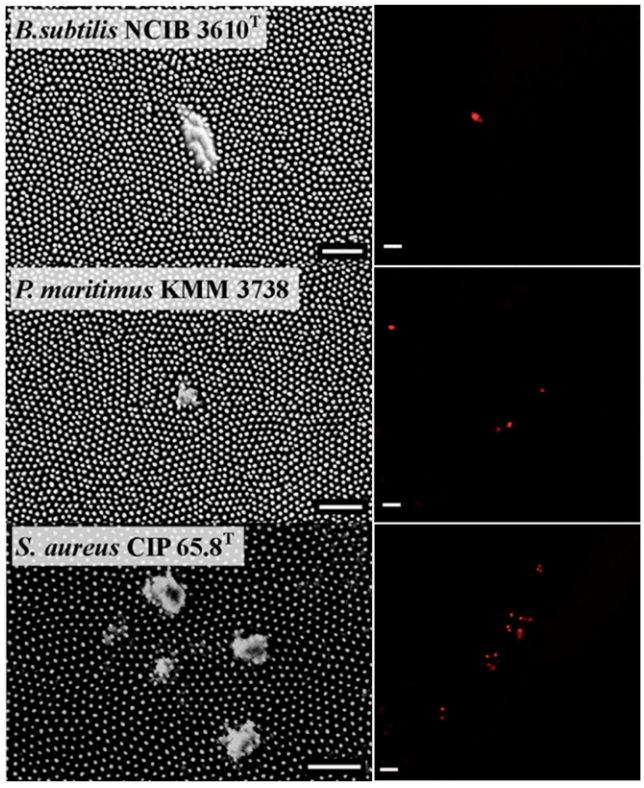

FIGURE 4 Cell interactions of surface-resistant *B. subtilis* NCIMB 3610T, *Planococcus maritimus* KMM 3738, and *S. aureus* CIP 65.8T strains after MW irradiation. All three strains were rendered susceptible to the action of the wing surface by MW treatment. Typical scanning electron micrographs (*left*) show substantial deformation of the cell morphologies of all three species. A CLSM viability analysis (*right*) shows that all cells were inactivated (shown in *red*).

bactericidal action of the wing surface. Subsequent viability experiments confirmed that the cells were indeed inactivated (Fig. 4, *right*). This is compelling evidence in support of the proposed model, confirming that the primary factors that determine the vulnerability of bacteria to the action of the wing surface are the mechanical properties of the membranes (i.e., the rigidity and initial stretching).

CONCLUSIONS

We developed a biophysical model of the interaction of bacterial cells with superhydrophobic nanopillar structures on the surface of cicada wings to provide a fundamental understanding of the mechanisms behind the recently discovered phenomenon of the bactericidal action of cicada wings. As the bacterial cells adsorb onto the nanopillar structures present on the wing surfaces, the cell membrane stretches in the regions suspended between the pillars. If the degree of stretching is sufficient, this will lead to cell rupture. Due to their greater rigidity, Gram-positive cells have a greater natural resistance to this effect than do Gram-negative cells. However, by decreasing their internal turgor pressure and hence their initial stretching and (to some degree) rigidity through MW irradiation, one can render these cells sensitive to the bactericidal mechanisms of the wing surfaces. Designing bio/nanomaterials that possess cicada-wing-like structures may be a promising avenue of research for applications in which minimizing bacterial contamination/infection is desirable.

This research was funded in part by the Advanced Manufacturing Co-operative Research Centre.

REFERENCES

1. Marmur, A. 2004. The Lotus effect: superhydrophobicity and metastability. *Langmuir.* 20:3517–3519.
2. Su, Y., B. Ji, …, K. C. Hwang. 2010. Nature's design of hierarchical superhydrophobic surfaces of a water strider for low adhesion and low-energy dissipation. *Langmuir.* 26:18926–18937.
3. Bhushan, B., and Y. C. Jung. 2011. Natural and biomimetic artificial surfaces for superhydrophobicity, self-cleaning, low adhesion, and drag reduction. *Prog. Mater. Sci.* 56:1–108.
4. Guo, Z., W. Liu, and B.-L. Su. 2011. Superhydrophobic surfaces: from natural to biomimetic to functional. *J. Colloid Interface Sci.* 353:335–355.
5. Webb, H. K., J. Hasan, …, E. P. Ivanova. 2011. Nature inspired structured surfaces for biomedical applications. *Curr. Med. Chem.* 18:3367–3375.
6. Bechert, D. W., M. Bruse, and W. Hage. 2000. Experiments with three-dimensional riblets as an idealized model of shark skin. *Exp. Fluids.* 28:403–412.
7. Chung, K. K., J. F. Schumacher, …, A. B. Brennan. 2007. Impact of engineered surface microtopography on biofilm formation of *Staphylococcus aureus*. *Biointerphases.* 2:89–94.
8. Ivanova, E. P., J. Hasan, …, R. J. Crawford. 2012. Natural bactericidal surfaces: mechanical rupture of *Pseudomonas aeruginosa* cells by cicada wings. *Small.* 8:2489–2494.
9. Fang, Y., G. Sun, …, L. Ren. 2007. Hydrophobicity mechanism of non-smooth pattern on surface of butterfly wing. *Chin. Sci. Bull.* 52: 711–719.
10. Watson, G. S., B. W. Cribb, and J. A. Watson. 2010. How micro/nano-architecture facilitates anti-wetting: an elegant hierarchical design on the termite wing. *ACS Nano.* 4:129–136.
11. Gao, X., X. Yan, …, L. Jiang. 2007. The dry-style antifogging properties of mosquito compound eyes and artificial analogues prepared by soft lithography. *Adv. Mater.* 19:2213–2217.
12. Mahdavi, A., L. Ferreira, …, J. M. Karp. 2008. A biodegradable and biocompatible gecko-inspired tissue adhesive. *Proc. Natl. Acad. Sci. USA.* 105:2307–2312.
13. Barthlott, W., and C. Neinhuis. 1997. Purity of the sacred lotus, or escape from contamination in biological surfaces. *Planta.* 202:1–8.
14. Bhushan, B., Y. C. Jung, …, K. Koch. 2009. Lotus-like biomimetic hierarchical structures developed by the self-assembly of tubular plant waxes. *Langmuir.* 25:1659–1666.
15. Koch, K., and W. Barthlott. 2009. Superhydrophobic and superhydrophilic plant surfaces: an inspiration for biomimetic materials. *Philos. Transact. A Math. Phys. Eng. Sci.* 367:1487–1509.
16. Koch, K., B. Bhushan, …, W. Barthlott. 2009. Fabrication of artificial lotus leaves and significance of hierarchical structure for superhydrophobicity and low adhesion. *Soft Matter.* 5:1386–1393.
17. Erbil, H. Y., A. L. Demirel, …, O. Mert. 2003. Transformation of a simple plastic into a superhydrophobic surface. *Science.* 299: 1377–1380.
18. Alves, N. M., J. Shi, …, J. F. Mano. 2009. Bioinspired superhydrophobic poly(L-lactic acid) surfaces control bone marrow derived cells adhesion and proliferation. *J. Biomed. Mater. Res. A.* 91:480–488.
19. Nosonovsky, M., V. Hejazi, …, P. K. Rohatgi. 2011. Metal matrix composites for sustainable lotus-effect surfaces. *Langmuir.* 27:14419–14424.
20. Kirschner, C. M., and A. B. Brennan. 2012. Bio-inspired antifouling strategies. *Ann. Rev. Mater. Res.* 42:8.1–8.19.
21. Hasan, J., H. K. Webb, …, E. P. Ivanova. 2012. Selective bactericidal activity of nano-patterned superhydrophobic cicada *Psaltoda claripennis* wing surfaces. *Appl. Microbiol. Biotechnol.* Dec 19. [Epub ahead of print].
22. Hong, S.-H., J. Hwang, and H. Lee. 2009. Replication of cicada wing's nano-patterns by hot embossing and UV nanoimprinting. *Nanotechnology.* 20:385303.
23. Zhang, G., J. Zhang, …, H. Shao. 2006. Cicada wings: a stamp from nature for nanoimprint lithography. *Small.* 2:1440–1443.
24. Shamis, Y., A. Taube, Y. Shramkov, N. Mitik-Dineva, B. Vu, and E. P. Ivanova. 2008. Development of a microwave treatment technique for bacterial decontamination of raw meat. *Int. J. Food Eng.* 4:8.
25. Yao, X., J. Walter, …, T. J. Beveridge. 2002. Atomic force microscopy and theoretical considerations of surface properties and turgor pressures of bacteria. *Colloids Surf. B Biointerfaces.* 23:213–230.
26. Whatmore, A. M., and R. H. Reed. 1990. Determination of turgor pressure in *Bacillus subtilis*: a possible role for K+ in turgor regulation. *J. Gen. Microbiol.* 136:2521–2526.
27. Arnoldi, M., M. Fritz, …, A. Boulbitch. 2000. Bacterial turgor pressure can be measured by atomic force microscopy. *Phys. Rev. E Stat. Phys. Plasmas Fluids Relat. Interdiscip. Topics.* 62(1 Pt B):1034–1044.
28. Shamis, Y., A. Taube, …, E. P. Ivanova. 2011. Specific electromagnetic effects of microwave radiation on *Escherichia coli*. *Appl. Environ. Microbiol.* 77:3017–3022.
29. Shamis, Y., S. Patel, …, E. P. Ivanova. 2009. A new sterilization technique of bovine pericardial biomaterial using microwave radiation. *Tissue Eng. Part C Methods.* 15:445–454.